

## 2D and 3D cartilage model platforms for drug evaluation and high-throughput screening assays

Foster, Nicky; Hall, Nicole M; El Haj, Alicia

DOI:

[10.1089/ten.TEB.2020.0354](https://doi.org/10.1089/ten.TEB.2020.0354)

License:

None: All rights reserved

*Document Version*

Peer reviewed version

*Citation for published version (Harvard):*

Foster, N, Hall, NM & El Haj, A 2021, '2D and 3D cartilage model platforms for drug evaluation and high-throughput screening assays', *Tissue Engineering Reviews: Part B*. <https://doi.org/10.1089/ten.TEB.2020.0354>

[Link to publication on Research at Birmingham portal](#)

### **Publisher Rights Statement:**

Final publication is available from Mary Ann Liebert, Inc., publishers <https://doi.org/10.1089/ten.TEB.2020.0354>

### **General rights**

Unless a licence is specified above, all rights (including copyright and moral rights) in this document are retained by the authors and/or the copyright holders. The express permission of the copyright holder must be obtained for any use of this material other than for purposes permitted by law.

- Users may freely distribute the URL that is used to identify this publication.
- Users may download and/or print one copy of the publication from the University of Birmingham research portal for the purpose of private study or non-commercial research.
- User may use extracts from the document in line with the concept of 'fair dealing' under the Copyright, Designs and Patents Act 1988 (?)
- Users may not further distribute the material nor use it for the purposes of commercial gain.

Where a licence is displayed above, please note the terms and conditions of the licence govern your use of this document.

When citing, please reference the published version.

### **Take down policy**

While the University of Birmingham exercises care and attention in making items available there are rare occasions when an item has been uploaded in error or has been deemed to be commercially or otherwise sensitive.

If you believe that this is the case for this document, please contact [UBIRA@lists.bham.ac.uk](mailto:UBIRA@lists.bham.ac.uk) providing details and we will remove access to the work immediately and investigate.

1 2D and 3D cartilage model platforms for drug  
2 evaluation and high-throughput screening assays

3 **Author 1:** Nicola C Foster, BSc (hons), MSc, PhD\*

4 Healthcare Technologies Institute, Institute of Translational Medicine, University of Birmingham,  
5 Edgbaston, B15 2TH

6 [N.C.Foster@bham.ac.uk](mailto:N.C.Foster@bham.ac.uk)

7 **Author 2:** Nicole M Hall

8 Division of Biomedical Engineering, James Watt School of Engineering, University of Glasgow,  
9 Glasgow, United Kingdom

10 [2255867H@student.gla.ac.uk](mailto:2255867H@student.gla.ac.uk)

11 **Author 3:** Alicia J El Haj, FREng, FRSB, FEAMBES

12 Healthcare Technologies Institute, Institute of Translational Medicine, University of Birmingham,  
13 Edgbaston, B15 2TH

14 [A.ElHaj@bham.ac.uk](mailto:A.ElHaj@bham.ac.uk)

15 **Key words:** articular cartilage, high-throughput screening assays, osteoarthritis, chondrogenesis,  
16 tissue engineering, drug evaluation

17 **Running title:** High throughput screening for cartilage

18 \* Corresponding author

## 19 Abstract

20 Osteoarthritis (OA) is a severely painful and debilitating disease of the joint, which brings about  
21 degradation of the articular cartilage and currently has few therapeutic solutions. 2-dimensional (2D)  
22 high-throughput screening assays have been widely used to identify candidate drugs with therapeutic  
23 potential for the treatment of OA. A number of small molecules which improve the chondrogenic  
24 differentiation of progenitor cells for tissue engineering applications have also been discovered in this  
25 way. However, due to the failure of these models to accurately represent the native joint  
26 environment, the efficacy of these drugs has been limited *in vivo*. Screening systems utilizing 3-  
27 dimensional (3D) models, which more closely reflect the tissue and its complex cell and molecular  
28 interactions, have also been described. However, the vast majority of these systems fail to recapitulate  
29 the complex, zonal structure of articular cartilage and its unique cell population. This review  
30 summarizes current 2D high throughput screening (HTS) techniques and addresses the question of  
31 how to use existing 3D models of tissue engineered cartilage to create 3D drug screening platforms  
32 with improved outcomes.

### 33 Impact statement

34 Currently, the use of 2D screening platforms in drug discovery is common practice. However, these  
35 systems often fail to predict efficacy *in vivo*, as they do not accurately represent the complexity of the  
36 native 3D environment. This article describes existing 2D and 3D high throughput systems used to  
37 identify small molecules for OA treatment or *in vitro* chondrogenic differentiation, and suggests ways  
38 to improve the efficacy of these systems based on the most recent research.

## 39 Introduction

40 2D high-throughput screening (HTS) assays have been widely used to test compounds for therapeutic  
41 potential for the treatment of OA. However, success has been limited due to the failure of these  
42 models to accurately represent the *in vivo* environment. As a result, some groups have developed 3D  
43 models, which simulate native cartilage tissue and its complex cell and molecular interactions more  
44 accurately. This review summarises the current state-of-the-art 2D and 3D high-throughput systems  
45 for cartilage drug screening (figure 1), and addresses the question of how to use 3D models of tissue  
46 engineered cartilage to create screening platforms with improved outcomes. Future steps needed for  
47 improved 3D models will be identified.

## 48 2D screening platforms

49 Cartilage has good phenotypic outcomes which are amenable to screening platforms. For example,  
50 the expression of type II collagen, aggrecan and sulphated glycosaminoglycans (sGAG) in the matrix  
51 are easily detected with a range of assays or dyes, and measurable alterations in its mechanical  
52 properties occur as a result of pathology or aberrant development <sup>1</sup>. Cell-based assays, involving the  
53 application of robotics and multi-well plates to screen vast libraries of chemical compounds for a  
54 potential effect on an identified target or pathway <sup>2,3</sup>, are a cornerstone of the drug discovery and  
55 approval process. Similarly, though often on smaller scale, such screening methods have identified  
56 small molecules which have generated much interest in the field of cartilage tissue engineering by  
57 drastically improving the chondrogenic differentiation and/or anabolic activity of precursor cells and  
58 chondrocytes.

59 Small molecules offer significant advantages over the growth factors and cytokines traditionally used  
60 to direct stem cell fate – the most notable being reproducibility, reduced immunogenicity, reduced  
61 manufacturing costs, improved stability (owing to low order structure) and avoidance of xenogeneic

62 sources <sup>4</sup>. In addition, rapid HTS allows for repurposing of small molecules with existing FDA approval  
63 which possess some hitherto unknown beneficial effect on catabolic pathways associated with joint  
64 pathogenesis or on cellular differentiation/anabolic activity. Add to that the reproducibility of these  
65 substances and the resultant implications for adopting Good Manufacturing Practice (GMP), and this  
66 renders therapies exploiting small molecules more amenable to clinical translation. Instead of utilising  
67 growth factors with known modes of action in relevant cell signalling pathways, the focus is now very  
68 much on identifying small molecules which act as agonists or antagonists of those pathways, and 2D  
69 screening platforms are a rapid and cost-effective means of doing so.

## 70 Cell sources for HTS

71 Primary chondrocytes appear to be the obvious cell choice for 2D screening assays seeking to identify  
72 novel modifiers of anabolic/catabolic response. Unfortunately, the issue of de-differentiation during  
73 the extensive cell number expansion period required for significant scale-up limits the usefulness of  
74 these cells in HTS platforms. Chondrocyte de-differentiation in monolayer culture is a well-established  
75 phenomenon, characterised by changes in morphology (from a rounded to a more fibroblastic  
76 structure) and reduction in the expression of makers such as aggrecan and type II collagen, with  
77 concomitant increases in expression of type I collagen <sup>5,6</sup>. Though some studies have utilized primary  
78 chondrocytes in 2D screening assays <sup>7-9</sup>, others have opted for induced cartilage models <sup>10</sup> or  
79 chondrogenic cell lines <sup>11,12</sup>. A recent study used the T/C28a2 cell line, in conjunction with automated  
80 liquid handling and high content screening, to test 1120 compounds for potential effectors of  
81 senescence and autophagy <sup>9</sup> (both associated with OA). For such large-scale screens, sufficient cell  
82 numbers would be difficult to obtain without the use of a cell line, although pluripotent cells may offer  
83 an alternative.

84 Interestingly, the majority of studies screening for potential novel inducers of chondrogenic  
85 differentiation opt for bone marrow stromal cells (BMSC) as the cellular component of their platform.

86 Presumably this is due to their well-documented chondrogenic potential <sup>13-15</sup>, high proliferative  
87 capacity <sup>16</sup> and the relative ease with which they can be isolated <sup>13</sup>. In addition, safety and efficacy has  
88 been shown in a number of clinical trials <sup>17</sup> utilising BMSC and they have demonstrated immune-  
89 modulatory and anti-inflammatory effects <sup>18</sup>. However, chondrogenic differentiation of these cells  
90 requires external media induction and there is a large body of evidence (reviewed elsewhere) to  
91 suggest that they are not able to produce hyaline cartilage <sup>19</sup>. A screening platform incorporating the  
92 cartilage superficial zone-resident progenitors would be more relevant, although limited availability  
93 of these cells would pose a barrier to high scale-up.

94 CRISPR gene editing allows for rapid and precise manipulation of target alleles without the risk of  
95 tumorigenicity associated with previously favoured modalities <sup>20,21</sup>. This technology could be utilised  
96 to overcome some of the barriers to scale-up by generating stem cells with reduced susceptibility to  
97 senescence <sup>22,23</sup> and increased differentiation potential <sup>24</sup>, or by triggering the re-differentiation of  
98 expanded chondrocytes <sup>25</sup>, all of which would aid the production of more relevant screening models.

## 99 [Simple 2D screening platforms](#)

100 2D screening platforms have yielded a number of promising candidates for cartilage tissue engineering  
101 and for tissues with a similar developmental lineage (table 1). Small molecules with therapeutic  
102 potential for cartilage repair have also been identified, including BNTA <sup>11</sup>, licofelone <sup>26,27</sup> and balicatib  
103 <sup>4,28</sup>. Kartogenin (KGN), developed by the Novartis Research Foundation <sup>29</sup>, is one of the more successful  
104 examples and demonstrates how effective simple HTS can be. In this system 22,000 heterocyclic  
105 molecules were screened using a 384-well format seeded with human BMSC; the presence of  
106 chondrogenic nodules, stained with rhodamine B and identified with simple light microscopy, revealed  
107 a “hit”. This small molecule was also shown to promote an early cell condensation phenotype and  
108 production of cartilage specific markers collagen type II and sex determining region Y-box 9 (SOX9).

109 Since then, a number of groups have confirmed its beneficial effects on chondrogenic differentiation  
110 *in vitro*<sup>30-32</sup> and reported promising outcomes in small animal cartilage injury models<sup>30,32</sup>.

111 The simplest 2D models comprise monolayer cell culture, with the addition of a molecule/molecular  
112 library to the culture medium and measurement of a simple output via a microplate reader or  
113 microscope. Choi et al.<sup>33</sup> wished to demonstrate that they could create a synthetic sulphonamide  
114 analogue of a protein kinase A inhibitor (the commercially available H-89), which had previously been  
115 shown to induce chondrogenic differentiation in rodent BMSC<sup>34</sup>. In this model, human adipose-  
116 derived stem cells (ASC) were seeded into individual 60 mm dishes and cultured for 11 days with their  
117 in-house library of H-89 analogues. Aggrecan protein expression was subsequently assessed via an  
118 enzyme-linked immunosorbent assay (ELISA) and “compound 6” was identified as a novel  
119 chondrogenic inducer<sup>33</sup>. Though this system proved effective on a small-scale with a known target, it  
120 does not lend itself to HTS and would be too laborious for a larger number of candidate molecules.  
121 Nevertheless, these simple screening systems are widely adopted in research institutes and  
122 undoubtedly have their place. Scaling up of such systems, with the use of multi-well plates and  
123 multichannel pipettes (or even robotic liquid handling systems) is also fairly commonplace. Shi et al.  
124<sup>11</sup> managed to screen 2320 natural and synthetic small compounds using a 96-well format seeded with  
125 a murine chondrogenic cell line. Again, cells were seeded in monolayer and molecules were added to  
126 the growth medium; proteoglycan production was assessed after 5 days via Alcian Blue staining and  
127 simple light microscopy. Though labour-intensive, this initial screening represents the limit of  
128 automation that many labs can achieve and allowed for a rapid narrowing of the number of candidate  
129 compounds, which were interrogated with increasingly complex and rigorous methods until BNTA was  
130 identified as a potential therapeutic agent for OA.

131 Despite initial excitement following the discovery of the molecule described above, none currently  
132 have market approval for the treatment of OA. Licofelone completed phase III clinical trials over a  
133 decade ago but, owing to inconclusive results, was never submitted for regulatory approval<sup>35,36</sup>. Trials



134 with Balicatib were terminated after completion of phase II when an increased risk of cardiovascular  
135 events was reported in patients receiving the drug <sup>37</sup>. KGN is currently undergoing phase II studies for  
136 the treatment of OA, with results anticipated in late 2021 <sup>38(p2)</sup>. SM04690, a Wnt pathway inhibitor  
137 whose chondroinductive properties were again identified with the aid of HTS <sup>10</sup>, is now in phase III  
138 clinical trials for the treatment of knee OA <sup>39</sup>.

### 139 [Advanced 2D screening platforms](#)

140 Some groups have sought to increase the physiological relevance of their 2D screening systems by  
141 introducing an extra level of complexity. One study reported the use of a microfluidics device to  
142 determine the optimum concentration of their candidate drug resveratrol for the proliferation of  
143 primary rodent chondrocytes <sup>8</sup>. As a system for optimising the dose of a drug with known benefits,  
144 this technique offers some useful insight; the authors presumably wished to increase proliferation of  
145 terminally differentiated chondrocytes for subsequent use in their animal model. However,  
146 proliferation is not the primary desirable outcome of a chondroinductive molecule and may come at  
147 the expense of cartilaginous matrix production <sup>40</sup>. Therefore, for a chondrogenic screening model,  
148 alternative outputs such as sGAG production would have been more relevant. Gradients do have well  
149 established physiological relevance, however <sup>41</sup>, and the use of microfluidics to create them can be of  
150 great benefit in screening systems. However, production of these (usually) bespoke systems is costly,  
151 time-consuming, and rarely compatible with commercially available liquid handling systems, thus  
152 presenting barriers to scale-up.

153 Another means of increasing the physiological relevance of 2D screening platforms is to introduce  
154 extracellular matrix (ECM)-mimicking chemical and mechanical properties. A number of these  
155 systems, though designed for other tissue types, could easily be adapted for cartilage screening  
156 models <sup>42,43</sup>. Others have sought to bridge the gap between 2D and 3D screening platforms by creating  
157 hydrogels with tuneable chemical and mechanical properties onto which cells can be seeded <sup>7,44,45</sup>. To

158 date this has not been attempted for cartilage screening models, but would be a useful addition to  
159 protocols as chondrocytes are known to be mechanoresponsive <sup>46</sup>.

## 160 Limitations of 2D platforms

161 2D screening systems offer numerous advantages and will undoubtedly continue to prove useful in  
162 both research environments the pharmaceutical industry. However, there are a number of well-  
163 documented limitations to these systems and candidate molecules, which initially appear promising,  
164 often fail to perform *in vivo*. Cells cultured in 3D are exposed to a microenvironment which more  
165 closely mimics the native tissue from which they are derived – in addition to the obvious geometrical  
166 parallels, they are exposed to paracrine signals from neighbouring cells, more comparable mechanical  
167 properties, and concentration gradients of growth factors, cytokines, nutrition and oxygen. It has also  
168 been well-documented in tumour models that cells cultured in 3D conditions demonstrate reduced  
169 drug sensitivity and require dosages that may be orders of magnitude higher than their monolayer  
170 counterparts <sup>47-49</sup>. ECM sequestering of soluble factors <sup>50</sup> and reduced mass transfer to the deeper  
171 regions of constructs <sup>47</sup> are likely to account for this observation. Whatever the mechanism, it is clear  
172 that dosage ranges determined from 2D screening platforms are unlikely to prove effective *in vivo*.  
173 Additionally, 2D models do not allow for the application of physiologically relevant mechanical  
174 stimulation during the culture period or for the use of changes in mechanical properties as an output  
175 measure. Given that cartilage is adept at withstanding a relentlessly harsh dynamic environment <sup>51</sup>,  
176 these are important considerations for anyone seeking to create a reliable *in vitro* model.

## 177 3D screening platforms

178 3D models can reflect the spatial relationships between cells at different stages of differentiation in  
179 their extracellular matrix and more closely represent systems and functions in the human body <sup>52</sup>. A  
180 recent review of the benefits of 3D culture concluded that it generally results in improved  
181 differentiation, protein/gene expression, viability and drug susceptibility compared to monolayer

182 culture; and when it comes to translating the findings of *in vitro* work to *in vivo* applications, 3D  
183 systems invariably perform better<sup>53</sup>. Cell-cell and cell-matrix interactions change dramatically when  
184 cells are taken from their native tissue to a 2D culture system where they are forced to adapt to a flat,  
185 smooth and extremely rigid surface; therefore, it is no surprise that effects observed under these  
186 conditions are often lost upon transfer to a more physiologically relevant microenvironment<sup>54</sup>.

187 Given that monolayer screening platforms often fail to predict efficacy *in vivo*, a number of groups  
188 have sought to develop systems which recapitulate some of the tissue's native architecture while  
189 allowing for large-scale and rapid outcomes (table 2). This is no trivial task and, while many of these  
190 models are unlikely to be adopted by the pharmaceutical industry without further development, they  
191 have proven invaluable in research settings and offer a way forward in terms of reducing the need for  
192 animal models. The number of models designed to probe for potential cartilage therapies/inducers of  
193 differentiation are relatively small, but many of the systems designed for other tissues could easily be  
194 adapted for chondrogenic applications.

195 Disease models are often adopted for the screening of potential novel therapeutic molecules, as  
196 changes in pathogenesis are relatively straightforward to detect via histology or gene/protein  
197 expression analysis. *In vitro* OA models can be chemically induced via cytokines or collagenases<sup>55,56</sup>,  
198 mechanically induced with the application of injurious strains<sup>55,56</sup>, or generated from chondrocytes  
199 donated by OA patients (with obvious limitations)<sup>57</sup>. Mechanically induced models, analogous to post-  
200 traumatic OA, are a useful tool but do not offer much insight into the earlier stages of pathology,  
201 whereas chemically-induced models require a combination of factors at a range of carefully controlled  
202 concentrations and exposure times to be truly representative<sup>56</sup>. There are a large number of genetic  
203 risk factors associated with OA susceptibility including *interleukin 1 beta (IL-1 $\beta$ )*, *hyaluronan synthase*  
204 *2 (HAS2)*, *lubricin*, *matrix metalloproteinase 13 (MMP13)* and *connexin 43 (CX43)*<sup>21</sup>. CRISPR gene  
205 editing technology has been used to ablate expression of these alleles for tissue engineering purposes  
206<sup>22,25,58-60</sup>, but could be used to increase the expression of disease-linked alleles in order to create

207 precision cellular models<sup>61</sup> which allow interrogation of the earlier stages of OA and identification of  
208 novel effectors of early pathogenesis.

### 209 High-throughput production of 3D cartilage models

210 Despite the many advantages of 3D culture, it is more labour-intensive and, in the case of spheroid  
211 production, requires large cell numbers. This is especially problematic for high-throughput  
212 applications where speed is paramount and large numbers of uniform constructs are required. A  
213 number of groups have developed high-throughput systems for generating cartilage micro-  
214 aggregates, which are readily compatible with standard micro-well plates<sup>62-65</sup>. Conical microwells can  
215 be fabricated from non-adherent materials such as agarose<sup>62,64</sup> or PDMS<sup>63</sup> with the aid of a rigid  
216 negative template and then punched into discs which fit easily into multi-well tissue culture plates.  
217 Primary chondrocytes<sup>62,64</sup> and BMSC<sup>63</sup> seeded into these micro-wells have been shown to perform at  
218 least as well as traditional spheroids in terms of chondrogenic matrix production and gene expression,  
219 and far better than monolayer culture where dedifferentiation to a fibroblastic phenotype is usually  
220 observed. In addition, the number of cells required to produce these micro-aggregates ranges from  
221 5000<sup>63</sup> down to 100<sup>62</sup> – a significant reduction from the 200,000 minimum required to form larger  
222 pellets. One issue with these microscale cultures is the potential for aggregates to move out of their  
223 wells during medium changes. Futrega et al. overcame this problem by placing a nylon mesh over their  
224 PDMS discs, the pores of which were sufficient to admit single cells during seeding but small enough  
225 to prevent the loss of the multicellular aggregates that subsequently formed<sup>63</sup>. Another group  
226 generated large numbers of columnar cartilage aggregates, by culturing and differentiating adipose-  
227 derived stem cells inside the PLA-coated pores of poly(L-glutamic acid)/adipic acid hydrogels<sup>66</sup>. Cells,  
228 preferentially bound to the PLA, gradually released thiol-containing molecules, which cleaved the PLA  
229 and enabled them to detach and formation aggregates.

230 Although spheroids lend themselves well to scaled-up fabrication, hydrogels allow for better mass  
231 transfer and can mimic the endogenous ECM more closely; therefore, a high-throughput system for  
232 producing cartilaginous hydrogels may be more appropriate for screening purposes. Witte et al.  
233 recently developed a microfluidics system for the rapid production of cell-laden alginate-fibronectin  
234 microgels <sup>65</sup>. Good viability, proliferation and production of chondrogenic markers were reported in  
235 both articular chondrocytes and BMSC encapsulated in the gels, however, as no monolayer or  
236 standard 3D controls were included, it is difficult to compare the performance of this model with lower  
237 throughput systems.

### 238 High density spheroid and micromass culture

239 For cartilage tissue engineering, spheroids (also referred to as pellets), being the most effective in  
240 terms of chondrogenic matrix production, are the gold standard. Unsurprisingly, therefore, this model  
241 has proven popular as a 3D screening platform for potential joint therapies and chondrogenic  
242 differentiation. Given their tumour-mimicking morphology, spheroids are also popular in cancer drug  
243 screening <sup>67,68</sup>. These self-assembling, cell-dense constructs are compatible with high-throughput due  
244 to the relative ease with which they can be formed in round bottom multi-well plates <sup>69</sup>. One  
245 consequence of spheroid culture (particularly those exceeding 500  $\mu\text{m}$  diameters <sup>70,71</sup>) is that  
246 nutrients and waste products are not able to diffuse evenly throughout the compact cell/ECM  
247 structure <sup>72</sup>. Though this often leads to compromised viability within the core of tumour spheroids <sup>71-</sup>  
248 <sup>73</sup>, hypoxic conditions (which mimic native articular cartilage) have actually been shown improve the  
249 expression of cartilage-specific markers in chondrogenic spheroids <sup>74-76</sup>.

250 The most basic (and arguably most scalable) attempts at creating 3D chondrogenic screening  
251 platforms have utilised high density culture of cell lines in multi-well plates. In an early example, Greco  
252 et al. added anabolic TGF $\beta$  or catabolic IL-1 $\beta$  to micromasses and investigated the effects of two anti-  
253 inflammatory drugs on sGAG accumulation and the expression of anabolic/catabolic genes <sup>77</sup>.

254 Although the outputs of this system were fairly low-throughput, other groups have increased the  
255 speed of data acquisition from standard sGAG and gene expression assays by performing them *in situ*,  
256 sometimes with the aid of liquid handling systems <sup>78,79</sup>.

257 Fluorescent reporter systems have also proven useful in spheroid-based platforms. Willard et al. used  
258 TGF $\beta$ -3 and murine tail fibroblast-derived induced pluripotent stem cells (iPSC), which had been pre-  
259 selected for *COL2A1* expression based on a green fluorescent protein (GFP) reporter system, to make  
260 pellets in a 96-well format <sup>79</sup>. Once formed, pellets were challenged with pro-inflammatory  
261 interleukin-1 $\alpha$  (IL-1 $\alpha$ ) to create a disease model. Five candidate OA drugs were incorporated into the  
262 model and sGAG loss to the medium was assessed via 1,9-Dimethyl-Methylene Blue (DMMB) assays,  
263 performed *in situ* in standard microplates. The relatively simple outputs of this platform lend  
264 themselves to scale-up and high-throughput, which makes it a promising alternative to standard 2D  
265 systems. However, the model takes over 5 weeks to set up and involves a degree of handling, wherein  
266 pellets are transferred to 96-well plates, which significantly reduces its appeal. In a simpler iteration,  
267 Dennis et al. recently used a fluorescent reporter system to screen for vitamins and minerals with the  
268 potential to enhance chondrogenic differentiation <sup>80</sup>. The use of a chondrogenic cell line, transformed  
269 with a collagen type II promoter-driven reporter system, provided a rapid output metric and facilitated  
270 the combinatorial screening of a large number of small molecules with anabolic potential.

271 Post-traumatic OA models can also be generated from spheroids with relative ease. Mohanraj et al.  
272 used a high-throughput device to mechanically challenge their constructs by applying injurious  
273 compressive force <sup>81</sup>. After the application of three potential therapeutic compounds, sGAG level was  
274 determined with DMMB assays and Alcian Blue staining. Unfortunately the outputs for this platform  
275 are laborious and the initial culture period is particularly lengthy; the only high-throughput aspect  
276 here is the application of injurious compressive force using an indentation device compatible with  
277 standard multi-well plates. Alcian Blue staining is tried and tested method of assessing the anabolic  
278 effects of compounds on chondrocytes, however, and can easily be adapted for high-throughput

279 systems. Parreno et al.<sup>82</sup> eluted the dye from their 96-well format screening platform and measured  
280 it spectrophotometrically via a microplate reader. Liquid handling systems, which are compatible with  
281 standard well-plates, could further increase the throughput of these models.

282 Spheroids recapitulate the key features of solid tumours, including geometry and limited mass transfer  
283 to the core region<sup>83</sup>. As such they have been successfully adopted in a number of screening platforms  
284 for potential cancer treatments<sup>84-88</sup>. Creation of spheroids from cancer cell lines via robotic liquid  
285 handling/automated pipetting systems in non-adherent 96-well<sup>85,86</sup> or 384-well<sup>88</sup> plates is a relatively  
286 straightforward and rapid process and such equipment, already heavily utilised by the pharmaceutical  
287 industry, is becoming more commonplace in research laboratories. These platforms are used to screen  
288 large libraries of potential chemotherapeutics and, where cell death/stunted growth is the primary  
289 goal, output measurements are easily generated with simple assays and microscopy techniques.  
290 Assessing the effects of small molecules on cartilage development or degradation requires more  
291 complexity in this regard, but nonetheless the design of these models could prove useful for this  
292 application. One group developed a two-phase system wherein cells were confined to a nanolitre-  
293 volume of dextran via droplet immersion into a well of poly(ethylene glycol) (PEG) solution and  
294 subsequently formed micro-aggregates<sup>86,88</sup>. This system is completely automated, compatible with  
295 96-<sup>86</sup> and 384-well<sup>88</sup> plates and can be adapted to include co-culture of multiple cell types, which  
296 would be an interesting avenue for models of cartilage given that endogenous tissue is in close  
297 proximity to the subchondral bone and its population of progenitor cells. Additionally, this model  
298 demonstrated that the effective dosage range of two commonly-used anti-cancer drugs was  
299 significantly higher for spheroids than for cells cultured in monolayer, reinforcing the importance of  
300 3D platforms which recapitulate the native ECM. Hanging droplets can also be used to produce large  
301 numbers of spheroids for screening purposes, either with the use of microfluidic systems<sup>84</sup> or  
302 microarray spotters<sup>87</sup>. However, these models usually require a degree of handling and/or the  
303 application of bespoke equipment, significantly reducing their throughput.

304 Lack of homogeneity in both size and shape of spheroids, is a common issue which can limit hinder  
305 the reproducibility of data for drug screening purposes <sup>89</sup>. The use of conical multi-well plates for  
306 generation of the constructs and the subsequent application of imaging software to select only the  
307 most spherical has been suggested by one group as the best means of eliminating variability <sup>89</sup>.  
308 Another study showed that spheroids generated from adipose derived stromal cells in non-adhesive  
309 hydrogel micro-moulds demonstrated homogeneous size and shape, while those formed using  
310 primary chondrocytes did not <sup>90</sup>. Therefore, spheroid uniformity is an important consideration for any  
311 groups seeking to utilise this model for HTS systems.

312 Another factor reducing the appeal of spheroids for screening purposes is the necessity for high cell  
313 numbers, which poses a significant barrier to scale-up. Huang et al. were able to adapt this model to  
314 an impressive 384-well format, using just 10,000 bovine BMSC per pellet, with the aid of an automated  
315 liquid dispensing device and a Breathe-Easy<sup>®</sup> sealing membrane to eliminate the requirement for  
316 medium changes <sup>78</sup>. Automated in-well digestion and DNA/sGAG assays were the primary output  
317 measures for this system, rendering it a truly high-throughput 3D screening platform.

318 In summary, spheroids are a sound 3D model for cartilage tissue engineering, which mimic the cell-  
319 cell and cell-ECM interactions of early development and have been shown enhance chondrogenic  
320 differentiation *in vitro* <sup>91</sup>. In addition, their relatively straightforward production and proven scalability  
321 mean they offer a promising alternative to existing 2D drug screening platforms. A spheroid-based  
322 screening platform, which produces uniform structures from a plentiful cell-source and utilises some  
323 of the rapid output measures outlined above, could offer a realistic alternative to the 2D platforms  
324 currently favoured by the pharmaceutical industry.

## 325 Hydrogels

326 Mature cartilage is a highly structured, viscoelastic material and markedly acellular compared to most  
327 tissues <sup>51,91,92</sup>. For these reasons a large number of studies have sought to create alternative 3D models



328 of cartilage from hydrogels, which mimic some of the tissue's key structural properties. In terms of  
329 predicting effective dosage ranges, there is also some evidence that these models are more effective  
330 than pellets; one study showed that oral cavity cancer cell-laden alginate displayed a chemo-sensitivity  
331 comparable to native tumour tissue, whereas cell-dense spheroids required significantly higher doses  
332 <sup>48</sup>.

333 A particular advantage of hydrogels is that their cell densities can be carefully controlled, which could  
334 be especially useful for models of cell-sparse tissues like articular cartilage. Simple hydrogel systems  
335 can easily be utilised for drug screening purposes <sup>93</sup> and rapid production of large numbers of cell-  
336 laden constructs has been demonstrated via droplet formation <sup>94-97</sup> or 3D printing <sup>98</sup>. Major drawbacks  
337 of droplet-based hydrogel systems, however, are that constructs are cultured together in one volume  
338 of medium and a high degree of liquid handling is required for processing. Large combinatorial  
339 hydrogels with gradients of tethered chemical ligands have also been used in high-throughput  
340 screening platforms <sup>99,100</sup>, but again constructs are cultured in a shared media pool, meaning that  
341 paracrine effects from neighbouring regions cannot be ruled out. To overcome this limitation, high-  
342 throughput microgel systems with discrete wells have also been utilised; although generation of these  
343 models requires access to expensive specialist equipment <sup>94</sup>.

344 Microfluidic devices have been used to culture hydrogels in dynamic conditions, thus creating shear  
345 forces and concentration gradients which help to recapitulate the endogenous environment. Li et al.  
346 <sup>101</sup> reported the use of such a device to screen the combinatorial effects of two growth factors on type  
347 II collagen production in Matrigel-encapsulated chondrocytes. Immunostaining of the entire  
348 polydimethylsiloxane (PDMS) chip, with the aid of image analysis software, allowed for rapid data  
349 acquisition. Accommodating just 3 culture chambers, this platform cannot be deemed high-  
350 throughput, but a scaled-up version of this technology could prove invaluable in determining the  
351 optimal concentration of small molecules with anabolic potential.

352 Recently the benefits of spheroids and hydrogels have been combined to create hybrid models,  
353 whereby small cell aggregates (as opposed to single cells) are encapsulated within hydrogels <sup>102</sup>. Kolb  
354 et al. developed a complex model in which aggregates of recombinant protein-expressing cell lines  
355 were co-encapsulated in PEG <sup>103</sup>. Used in conjunction with a reporter cell line that gives rapid outputs,  
356 this combinatorial microgel platform certainly lends itself to high-throughput systems and could easily  
357 be adapted for cartilage screening. However, initial generation of multiple protein-expressing cell lines  
358 is a lengthy process compared to standard screening methods and may deter interest from the  
359 pharmaceutical industry.

## 360 Organoids

361 Organoids are similar to spheroids, but are generally defined by three key features: they must be  
362 formed from multiple cell types or stages, must have some aspect or function of the tissue they are  
363 modelling and must develop following the same basic patterning <sup>104,105</sup>. There are well-described  
364 organoid models for tissues such as brain <sup>106</sup>, stomach <sup>107</sup> and liver <sup>108</sup> which fulfil all of these criteria.  
365 However, cartilage “organoids” are often simple spheroids composed of just one cell type. The  
366 distinction between spheroids and organoids is a difficult one to make with hyaline cartilage, which  
367 naturally comprises mainly one cell type and is a tissue (albeit a highly structured zonal one) rather  
368 than an organ, such as the brain. Though cartilaginous spheroids are sometimes referred to as  
369 “organoids”, for the purposes of this review the term “organoid” will be reserved for tissue with more  
370 complexity. Few attempts have been made to culture cartilage organoids with structures, cell densities  
371 and niche properties more characteristic of the native tissue than the high density pellet culture  
372 described above. In one example, however, O’Connor et al. created an osteochondral organoid, by  
373 using TGF $\beta$ -3 and bone morphogenetic protein 2 to mirror endochondral ossification in induced  
374 pluripotent stem cell (iPSC) micromasses <sup>109</sup>. Comprising a cartilaginous core with a calcified outer ring,  
375 this model could prove very useful for the screening of potential modifiers of OA, which is after all a  
376 disease of the entire joint, including the subchondral bone <sup>110,111</sup>. Although the 73-day culture period

377 is not ideally suited to high-throughput processes, the expansion capacity of iPSC is a real advantage  
378 in this regard. Furthermore, the use of these cells presents greater opportunity for conducting patient-  
379 and/or disease-specific drug screening.

### 380 [Cartilage-on-a-chip technology](#)

381 Organ-on-a-chip technology may be a promising alternative approach to the creation of 3D cartilage  
382 models, as it lends itself to the formation of stratified structures. As screening platforms, these niche-  
383 mimicking structures are also more likely to give meaningful results and reduce the risk of futile  
384 investment in fruitless products.

385 Rosser et al. recently described a system in which fibrin-encapsulated chondrocytes were loaded into  
386 3 mm semi-circular tissue chambers embedded into PDMS slabs <sup>112</sup>. A microfluidics system was used  
387 to drive medium past only the flat side of the chamber, thus creating cyclic shear forces and  
388 concentration gradients which mimicked the articular surface and underlying, avascular tissue. Cells  
389 in this system retained their rounded morphology and chondrogenic gene expression, unlike their  
390 monolayer counterparts. Incorporation of pro-inflammatory cytokines to the system demonstrated  
391 its potential as a screening platform, but output measures were relatively low-throughput. In a similar  
392 model, Ochetta et al. went a step further by incorporating a sub-chamber into their PDMS stamp to  
393 enable the application of confined compression, thereby generating the crucial mechanical stimulus  
394 to which the joint is subject <sup>113</sup>. Chondrocytes, encapsulated in PEG hydrogels, were loaded into the  
395 micro-chambers and high compressive loads were applied in order mimic OA pathogenesis. A range  
396 of commonly-used anti-inflammatory and anti-catabolic drugs were added to the medium for 3 days  
397 before tissue integrity was assessed with sGAG and matrix metalloproteinase 13 assays. This model is  
398 especially versatile, as compressive loads can be adjusted to recapitulate normal joint conditions for  
399 the purpose of screening potential chondrogenic/anabolic compounds. Both of these cartilage-on-a-  
400 chip systems utilise microfluidics technology to rapidly produce potentially large numbers of

401 chondrocyte-laden hydrogel constructs, which mimic not only the mechanical properties of articular  
402 cartilage but also its physiological gradients and dynamic environment. One drawback to this  
403 technology is the requirement for custom moulds which are not compatible with standard microplate  
404 readers and, therefore, not amenable to high-throughput assay-based outcomes. However, the PDMS  
405 stamps described here can be fabricated to match the dimensions of standard microscope slides,  
406 thereby allowing for the use of automated microscopy as a means of increasing the throughput of  
407 these systems.

408 Neither of the cartilage-on-a-chip models described above attempted to recreate the zonal  
409 compartmentalisation of articular cartilage, nor was inclusion of cells at different stages of  
410 differentiation considered. Lin et al.<sup>114</sup> addressed this issue by using iPSC to create an osteochondral  
411 “tissue chip”. iPSC-derived progenitors were encapsulated in gelatin and cultured in a dual flow  
412 bioreactor, whereby cells at the base of the construct were exposed to osteogenic cues and those at  
413 the top to chondrogenic cues, with a natural gradient across the depth of the gel akin to the native  
414 environment (figure 1E). After 28 days of culture, good expression of chondrogenic and osteogenic  
415 makers were seen in the upper and lower regions of the chip respectively; induction of an OA disease  
416 phenotype was then achieved with the addition of interleukin-1 $\beta$  (IL-1 $\beta$ ) to the medium for 7 days. By  
417 incorporating progenitor cells, multiple tissue types, dynamic conditions and tuneable concentration  
418 gradients, this model recapitulates the endogenous joint environment more closely than the vast  
419 majority described to date. To demonstrate its potential as a screening platform, the FDA-approved  
420 drug Celecoxib was administered to the system, resulting in significant decreases in expression of  
421 catabolic and inflammatory factors. This versatile model also has the potential to screen novel  
422 inducers of anabolic response in cartilage tissue, simply by omitting the IL-1 $\beta$  culture period. The  
423 authors do not comment on the capacity of this system for generating and maintaining large numbers  
424 of constructs, and the output measures adopted (primarily gene expression analysis) are not  
425 amenable to high-throughput. As a system for optimising the concentration of small molecules  
426 identified by other screening platforms, however, this model certainly holds great promise.

## 427 Outlook for 3D screening platforms

428 3D models, which more accurately recapitulate mature cell-cell and cell-ECM interactions and display  
429 patterns of spatial gene and protein expression more akin to the native tissue environment <sup>52</sup>, have  
430 gained popularity in recent years. In addition, a promising number of studies have demonstrated that  
431 high-throughput production of 3D cartilage models is possible and that rapid outputs are achievable  
432 with the aid of technology such as robotic liquid handling systems. Access to such technology poses  
433 no barrier for large pharmaceutical companies and is becoming more commonplace in smaller labs  
434 <sup>9,10,43,84,94,95</sup>. Nonetheless, 3D models require longer culture periods, are more labour-intensive and can  
435 lack the requisite reproducibility for scale up <sup>52</sup>. Models incorporating the full cascade of chondrocyte  
436 differentiation present *in vivo* are also lacking; a platform with such complexity might more accurately  
437 predict *in vivo* drug response, but would undoubtedly require greater investment of both time and  
438 funds. For smaller labs, where there is less emphasis on high-throughput, 3D platforms are widely  
439 utilised for small-scale screening and optimisation of established anabolic/catabolic agents. Complex  
440 models such as organoids are unlikely to be adopted by pharmaceutical companies in the near future  
441 for the screening of vast chemical libraries, however, large-scale spheroid culture <sup>78</sup> and high-  
442 throughput hydrogel production <sup>94</sup> offer a realistic alternatives to the inadequate 2D systems currently  
443 employed.

## 444 Conclusion

445 High-throughput screening platforms are essential for identifying small molecules with the potential  
446 to modify both chondrogenic differentiation and cartilage catabolic processes. 2D systems, which are  
447 economical, compatible with robotic liquid handling technology and offer rapid output metrics are  
448 currently favoured by the pharmaceutical industry. A number of potential disease-modifying OA drugs  
449 have been discovered in this way, as have molecules such as KGN, which hold great promise for  
450 cartilage tissue engineering. However, 2D culture systems do not reliably represent *in vivo* conditions

451 and often fail to predict efficacy in subsequent animal models. 3D models recapitulate the cell niche  
452 more closely, produce superior cartilage *in vitro* and show differential dose responses to disease  
453 modifying drugs. A range of 3D models (including spheroids, hydrogels and organ-on-a-chip) have  
454 been adapted to create screening platforms for cartilage and many other tissue types. Drawbacks of  
455 these systems include longer culture periods, necessity for higher cell numbers, increased handling  
456 and increased costs. However, in order to reduce the requirement for animal models and to limit  
457 wasted investment in ineffective drugs, it is essential that research institutes and the pharmaceutical  
458 industry alike move towards the use of effective 3D models for screening purposes and design new  
459 approaches which encapsulate the complexity of zonal structures and cell types within the cartilage  
460 matrix. If 3D platforms are to be adopted on a large-scale for pharmaceutical drug screening, economic  
461 considerations must be carefully balanced with the need for outcomes which accurately predict *in vivo*  
462 response. Initial investment in systems with more physiological relevance could ultimately mitigate  
463 the fruitless development of drugs which fail to obtain market approval.

## 464 Acknowledgements

## 465 Author(s') disclosure statement(s)

466 The authors declare no competing or financial interests.

## 467 Funding statement (see below)

468 The authors would like to thank the UK Regenerative Medicine Platform and the Medical Research  
469 Council for provision of funding.

## 470 References

- 471 1. Grogan SP, D’Lima DD. Joint aging and chondrocyte cell death. *Int J Clin Rheumatol*.  
472 2010;5(2):199-214. doi:10.2217/ijr.10.3
- 473 2. Tamimi NAM, Ellis P. Drug Development: From Concept to Marketing! *Nephron Clin Pract*.  
474 2009;113(3):c125-c131. doi:10.1159/000232592
- 475 3. Lo B, Field MJ. *The Pathway from Idea to Regulatory Approval: Examples for Drug*  
476 *Development*. National Academies Press (US); 2009. Accessed September 23, 2020.  
477 <https://www.ncbi.nlm.nih.gov/books/NBK22930/>
- 478 4. Lo KW-H, Jiang T, Gagnon KA, Nelson C, Laurencin CT. Small Molecule based Musculoskeletal  
479 Regenerative Engineering. *Trends Biotechnol*. 2014;32(2):74-81.  
480 doi:10.1016/j.tibtech.2013.12.002
- 481 5. Hong E, Reddi AH. Dedifferentiation and redifferentiation of articular chondrocytes from  
482 surface and middle zones: changes in microRNAs-221/-222, -140, and -143/145 expression.  
483 *Tissue Eng Part A*. 2013;19(7-8):1015-1022. doi:10.1089/ten.TEA.2012.0055
- 484 6. Charlier E, Deroyer C, Ciregia F, et al. Chondrocyte dedifferentiation and osteoarthritis (OA).  
485 *Biochem Pharmacol*. 2019;165:49-65. doi:10.1016/j.bcp.2019.02.036
- 486 7. Sharma S, Floren M, Ding Y, Stenmark KR, Tan W, Bryant SJ. A photoclickable peptide  
487 microarray platform for facile and rapid screening of 3-D tissue microenvironments.  
488 *Biomaterials*. 2017;143:17-28. doi:10.1016/j.biomaterials.2017.07.025
- 489 8. Ming L, Zhipeng Y, Fei Y, et al. Microfluidic-based screening of resveratrol and drug-loading  
490 PLA/Gelatin nano-scaffold for the repair of cartilage defect. *Artif Cells Nanomedicine*  
491 *Biotechnol*. 2018;46(sup1):336-346. doi:10.1080/21691401.2017.1423498
- 492 9. Nogueira-Recalde U, Lorenzo-Gómez I, Blanco FJ, et al. Fibrates as drugs with senolytic and  
493 autophagic activity for osteoarthritis therapy. *EBioMedicine*. 2019;45:588-605.  
494 doi:10.1016/j.ebiom.2019.06.049
- 495 10. Deshmukh V, Hu H, Barroga C, et al. A small-molecule inhibitor of the Wnt pathway (SM04690)  
496 as a potential disease modifying agent for the treatment of osteoarthritis of the knee.  
497 *Osteoarthritis Cartilage*. 2018;26(1):18-27. doi:10.1016/j.joca.2017.08.015
- 498 11. Shi Y, Hu X, Cheng J, et al. A small molecule promotes cartilage extracellular matrix generation  
499 and inhibits osteoarthritis development. *Nat Commun*. 2019;10(1):1914. doi:10.1038/s41467-  
500 019-09839-x
- 501 12. Le BQ, Fernandes H, Bouten CVC, Karperien M, van Blitterswijk C, de Boer J. High-Throughput  
502 Screening Assay for the Identification of Compounds Enhancing Collagenous Extracellular  
503 Matrix Production by ATDC5 Cells. *Tissue Eng Part C Methods*. 2015;21(7):726-736.  
504 doi:10.1089/ten.TEC.2014.0088
- 505 13. Johnstone B, Hering TM, Caplan AI, Goldberg VM, Yoo JU. In vitro chondrogenesis of bone  
506 marrow-derived mesenchymal progenitor cells. *Exp Cell Res*. 1998;238(1):265-272.  
507 doi:10.1006/excr.1997.3858

- 508 14. Johnstone B, Yoo JU. Autologous mesenchymal progenitor cells in articular cartilage repair. *Clin*  
509 *Orthop*. 1999;(367 Suppl):S156-162. doi:10.1097/00003086-199910001-00017
- 510 15. Pittenger MF, Mackay AM, Beck SC, et al. Multilineage potential of adult human mesenchymal  
511 stem cells. *Science*. 1999;284(5411):143-147. doi:10.1126/science.284.5411.143
- 512 16. McGonagle D, Baboolal TG, Jones E. Native joint-resident mesenchymal stem cells for cartilage  
513 repair in osteoarthritis. *Nat Rev Rheumatol*. 2017;13(12):719-730.  
514 doi:10.1038/nrrheum.2017.182
- 515 17. Yubo M, Yanyan L, Li L, Tao S, Bo L, Lin C. Clinical efficacy and safety of mesenchymal stem cell  
516 transplantation for osteoarthritis treatment: A meta-analysis. *PLoS One*. 2017;12(4):e0175449.  
517 doi:10.1371/journal.pone.0175449
- 518 18. Tyndall A. Mesenchymal stem cell treatments in rheumatology—a glass half full? *Nat Rev*  
519 *Rheumatol*. 2014;10(2):117-124. doi:10.1038/nrrheum.2013.166
- 520 19. Somoza RA, Welter JF, Correa D, Caplan AI. Chondrogenic Differentiation of Mesenchymal  
521 Stem Cells: Challenges and Unfulfilled Expectations. *Tissue Eng Part B Rev*. 2014;20(6):596-608.  
522 doi:10.1089/ten.teb.2013.0771
- 523 20. Guilak F, Piferdehirt L, Ross AK, et al. Designer stem cells: Genome engineering and the next  
524 generation of cell-based therapies. *J Orthop Res Off Publ Orthop Res Soc*. 2019;37(6):1287-  
525 1293. doi:10.1002/jor.24304
- 526 21. Tanikella AS, Hardy MJ, Frahs SM, et al. Emerging Gene-Editing Modalities for Osteoarthritis.  
527 *Int J Mol Sci*. 2020;21(17). doi:10.3390/ijms21176046
- 528 22. Fu L, Hu Y, Song M, et al. Up-regulation of FOXD1 by YAP alleviates senescence and  
529 osteoarthritis. *PLoS Biol*. 2019;17(4):e3000201. doi:10.1371/journal.pbio.3000201
- 530 23. Ren X, Hu B, Song M, et al. Maintenance of Nucleolar Homeostasis by CBX4 Alleviates  
531 Senescence and Osteoarthritis. *Cell Rep*. 2019;26(13):3643-3656.e7.  
532 doi:10.1016/j.celrep.2019.02.088
- 533 24. Perez-Pinera P, Kocak DD, Vockley CM, et al. RNA-guided gene activation by CRISPR-Cas9-based  
534 transcription factors. *Nat Methods*. 2013;10(10):973-976. doi:10.1038/nmeth.2600
- 535 25. Varela-Eirín M, Varela-Vázquez A, Guitián-Caamaño A, et al. Targeting of chondrocyte plasticity  
536 via connexin43 modulation attenuates cellular senescence and fosters a pro-regenerative  
537 environment in osteoarthritis. *Cell Death Dis*. 2018;9(12):1166. doi:10.1038/s41419-018-1225-  
538 2
- 539 26. Laufer S. Discovery and development of ML3000. *InflammoPharmacology*. 2001;9(1):101-112.  
540 doi:10.1163/156856001300248371
- 541 27. Raynauld J-P, Martel-Pelletier J, Bias P, et al. Protective effects of licofelone, a 5-lipoxygenase  
542 and cyclo-oxygenase inhibitor, versus naproxen on cartilage loss in knee osteoarthritis: a first  
543 multicentre clinical trial using quantitative MRI. *Ann Rheum Dis*. 2009;68(6):938-947.  
544 doi:10.1136/ard.2008.088732
- 545 28. Brömme D, Lecaille F. Cathepsin K inhibitors for osteoporosis and potential off-target effects.  
546 *Expert Opin Investig Drugs*. 2009;18(5):585-600. doi:10.1517/13543780902832661



- 547 29. Johnson K, Zhu S, Tremblay MS, et al. A stem cell-based approach to cartilage repair. *Science*.  
548 2012;336(6082):717-721. doi:10.1126/science.1215157
- 549 30. Zhang J, Wang JH-C. Kartogenin induces cartilage-like tissue formation in tendon-bone  
550 junction. *Bone Res*. 2014;2. doi:10.1038/boneres.2014.8
- 551 31. Spakova T, Plsikova J, Harvanova D, Lacko M, Stolfa S, Rosocha J. Influence of Kartogenin on  
552 Chondrogenic Differentiation of Human Bone Marrow-Derived MSCs in 2D Culture and in Co-  
553 Cultivation with OA Osteochondral Explant. *Mol J Synth Chem Nat Prod Chem*. 2018;23(1).  
554 doi:10.3390/molecules23010181
- 555 32. Liu C, Li T, Yang Z, et al. Kartogenin Enhanced Chondrogenesis in Cocultures of Chondrocytes  
556 and Bone Mesenchymal Stem Cells. *Tissue Eng Part A*. 2018;24(11-12):990-1000.  
557 doi:10.1089/ten.TEA.2017.0162
- 558 33. Choi E, Lee J, Lee S, et al. Potential therapeutic application of small molecule with sulfonamide  
559 for chondrogenic differentiation and articular cartilage repair. *Bioorg Med Chem Lett*.  
560 2016;26(20):5098-5102. doi:10.1016/j.bmcl.2016.08.069
- 561 34. Hwang K-C, Kim JY, Chang W, et al. Chemicals that modulate stem cell differentiation. *Proc Natl*  
562 *Acad Sci*. 2008;105(21):7467-7471. doi:10.1073/pnas.0802825105
- 563 35. Fischer L, Hornig M, Pergola C, et al. The molecular mechanism of the inhibition by licofelone  
564 of the biosynthesis of 5-lipoxygenase products. *Br J Pharmacol*. 2007;152(4):471-480.  
565 doi:10.1038/sj.bjp.0707416
- 566 36. Alvaro-Gracia JM. Licofelone—clinical update on a novel LOX/COX inhibitor for the treatment  
567 of osteoarthritis. *Rheumatology*. 2004;43(suppl\_1):i21-i25. doi:10.1093/rheumatology/keh105
- 568 37. Latourte A, Kloppenburg M, Richette P. Emerging pharmaceutical therapies for osteoarthritis.  
569 *Nat Rev Rheumatol*. Published online October 29, 2020:1-16. doi:10.1038/s41584-020-00518-6
- 570 38. Samumed LLC. *A Phase 2, 52-Week, Multicenter, Randomized, Double-Blind, Placebo-Controlled*  
571 *Study Evaluating the Safety, Tolerability, and Efficacy of Two Injections of SM04690 Injected in*  
572 *the Target Knee Joint of Moderately to Severely Symptomatic Osteoarthritis Subjects*.  
573 clinicaltrials.gov; 2020. Accessed October 28, 2020.  
574 <https://clinicaltrials.gov/ct2/show/NCT03727022>
- 575 39. Tattory M. Samumed Announces Positive End-of-Phase 2 Meeting with FDA for SM04690 in  
576 Knee Osteoarthritis. :2.
- 577 40. Wuelling M, Vortkamp A. Chondrocyte proliferation and differentiation. *Endocr Dev*.  
578 2011;21:1-11. doi:10.1159/000328081
- 579 41. Zhu D, Tong X, Trinh P, Yang F. Mimicking Cartilage Tissue Zonal Organization by Engineering  
580 Tissue-Scale Gradient Hydrogels as 3D Cell Niche. *Tissue Eng Part A*. 2018;24(1-2):1-10.  
581 doi:10.1089/ten.tea.2016.0453
- 582 42. Floren M, Tan W. Three-Dimensional, Soft Neotissue Arrays as High Throughput Platforms for  
583 the Interrogation of Engineered Tissue Environments. *Biomaterials*. 2015;59:39-52.  
584 doi:10.1016/j.biomaterials.2015.04.036

- 585 43. Gobaa S, Gayet RV, Lutolf MP. Artificial niche microarrays for identifying extrinsic cell-fate  
586 determinants. *Methods Cell Biol.* 2018;148:51-69. doi:10.1016/bs.mcb.2018.06.012
- 587 44. Rape AD, Zibinsky M, Murthy N, Kumar S. A synthetic hydrogel for the high-throughput study  
588 of cell-ECM interactions. *Nat Commun.* 2015;6:8129. doi:10.1038/ncomms9129
- 589 45. Tong X, Jiang J, Zhu D, Yang F. Hydrogels with Dual Gradients of Mechanical and Biochemical  
590 Cues for Deciphering Cell-Niche Interactions. *ACS Biomater Sci Eng.* 2016;2(5):845-852.  
591 doi:10.1021/acsbiomaterials.6b00074
- 592 46. Zhao Z, Li Y, Wang M, Zhao S, Zhao Z, Fang J. Mechanotransduction pathways in the regulation  
593 of cartilage chondrocyte homeostasis. *J Cell Mol Med.* 2020;24(10):5408-5419.  
594 doi:10.1111/jcmm.15204
- 595 47. Kapałczyńska M, Kolenda T, Przybyła W, et al. 2D and 3D cell cultures – a comparison of  
596 different types of cancer cell cultures. *Arch Med Sci AMS.* 2018;14(4):910-919.  
597 doi:10.5114/aoms.2016.63743
- 598 48. Hsieh C-H, Chen Y-D, Huang S-F, Wang H-M, Wu M-H. The effect of primary cancer cell culture  
599 models on the results of drug chemosensitivity assays: the application of perfusion  
600 microbio-reactor system as cell culture vessel. *BioMed Res Int.* 2015;2015:470283.  
601 doi:10.1155/2015/470283
- 602 49. Bulysheva AA, Bowlin GL, Petrova SP, Yeudall WA. Enhanced chemoresistance of squamous  
603 carcinoma cells grown in 3D cryogenic electrospun scaffolds. *Biomed Mater Bristol Engl.*  
604 2013;8(5):055009. doi:10.1088/1748-6041/8/5/055009
- 605 50. Griffith LG, Swartz MA. Capturing complex 3D tissue physiology in vitro. *Nat Rev Mol Cell Biol.*  
606 2006;7(3):211-224. doi:10.1038/nrm1858
- 607 51. Foster NC, Henstock JR, Reinwald Y, El Haj AJ. Dynamic 3D culture: models of chondrogenesis  
608 and endochondral ossification. *Birth Defects Res Part C Embryo Today Rev.* 2015;105(1):19-33.  
609 doi:10.1002/bdrc.21088
- 610 52. Kapałczyńska M, Kolenda T, Przybył W, et al. 2D and 3D Cell Cultures - A Comparison of  
611 Different Types of Cancer Cell Cultures. *Arch Med Sci.* 2016;14(4):910-919.  
612 doi:10.5114/aoms.2016.63743
- 613 53. Ravi M, Paramesh V, Kaviya SR, Anuradha E, Solomon FDP. 3D Cell Culture Systems:  
614 Advantages and Applications. *J Cell Physiol.* 2015;230(1):16-26. doi:10.1002/jcp.24683
- 615 54. Mazzoleni G, Di Lorenzo D, Steimberg N. Modelling tissues in 3D: the next future of pharmaco-  
616 toxicology and food research? *Genes Nutr.* 2009;4(1):13-22. doi:10.1007/s12263-008-0107-0
- 617 55. Cope PJ, Ourradi K, Li Y, Sharif M. Models of osteoarthritis: the good, the bad and the  
618 promising. *Osteoarthritis Cartilage.* 2019;27(2):230-239. doi:10.1016/j.joca.2018.09.016
- 619 56. Johnson CI, Argyle DJ, Clements DN. In vitro models for the study of osteoarthritis. *Vet J.*  
620 2016;209:40-49. doi:10.1016/j.tvjl.2015.07.011
- 621 57. Yeung P, Cheng KH, Yan CH, Chan BP. Collagen microsphere based 3D culture system for  
622 human osteoarthritis chondrocytes (hOACs). *Sci Rep.* 2019;9. doi:10.1038/s41598-019-47946-3

- 623 58. Farhang N, Brunger JM, Stover JD, et al. \* CRISPR-Based Epigenome Editing of Cytokine  
624 Receptors for the Promotion of Cell Survival and Tissue Deposition in Inflammatory  
625 Environments. *Tissue Eng Part A*. 2017;23(15-16):738-749. doi:10.1089/ten.TEA.2016.0441
- 626 59. Seidl CI, Fulga TA, Murphy CL. CRISPR-Cas9 targeting of MMP13 in human chondrocytes leads  
627 to significantly reduced levels of the metalloproteinase and enhanced type II collagen  
628 accumulation. *Osteoarthritis Cartilage*. 2019;27(1):140-147. doi:10.1016/j.joca.2018.09.001
- 629 60. Zhao L, Huang J, Fan Y, et al. Exploration of CRISPR/Cas9-based gene editing as therapy for  
630 osteoarthritis. *Ann Rheum Dis*. 2019;78(5):676-682. doi:10.1136/annrheumdis-2018-214724
- 631 61. Fellmann C, Gowen BG, Lin P-C, Doudna JA, Corn JE. Cornerstones of CRISPR-Cas in drug  
632 development and therapy. *Nat Rev Drug Discov*. 2017;16(2):89-100. doi:10.1038/nrd.2016.238
- 633 62. Moreira Teixeira LS, Leijten JCH, Sobral J, et al. High throughput generated micro-aggregates of  
634 chondrocytes stimulate cartilage formation in vitro and in vivo. *Eur Cell Mater*. 2012;23:387-  
635 399. doi:10.22203/ecm.v023a30
- 636 63. Futrega K, Palmer JS, Kinney M, et al. The microwell-mesh: A novel device and protocol for the  
637 high throughput manufacturing of cartilage microtissues. *Biomaterials*. 2015;62:1-12.  
638 doi:10.1016/j.biomaterials.2015.05.013
- 639 64. De Moor L, Beyls E, Declercq H. Scaffold Free Microtissue Formation for Enhanced Cartilage  
640 Repair. *Ann Biomed Eng*. 2020;48(1):298-311. doi:10.1007/s10439-019-02348-4
- 641 65. Witte K, Andres MC de, Wells JA, Dalby MJ, Salmeron-Sanchez M, Oreffo R. Chondrobags: a  
642 high throughput alginate-fibronectin micromass platform for in vitro human cartilage  
643 formation. *Biofabrication*. Published online 2020. doi:10.1088/1758-5090/abb653
- 644 66. Xiahou Z, She Y, Zhang J, et al. Designer Hydrogel with Intelligently Switchable Stem-Cell  
645 Contact for Incubating Cartilaginous Microtissues. *ACS Appl Mater Interfaces*.  
646 2020;12(36):40163-40175. doi:10.1021/acsami.0c13426
- 647 67. Fennema E, Rivron N, Rouwkema J, van Blitterswijk C, de Boer J. Spheroid culture as a tool for  
648 creating 3D complex tissues. *Trends Biotechnol*. 2013;31(2):108-115.  
649 doi:10.1016/j.tibtech.2012.12.003
- 650 68. Vasyutin I, Zerihun L, Ivan C, Atala A. Bladder Organoids and Spheroids: Potential Tools for  
651 Normal and Diseased Tissue Modelling. *Anticancer Res*. 2019;39(3).  
652 doi:10.21873/anticancer.13219
- 653 69. Abu-Hakmeh AE, Wan LQ. High-throughput cell aggregate culture for stem cell chondrogenesis.  
654 *Methods Mol Biol Clifton NJ*. 2014;1202:11-19. doi:10.1007/7651\_2014\_75
- 655 70. Sutherland RM, Sordat B, Bamat J, Gabbert H, Bourrat B, Mueller-Klieser W. Oxygenation and  
656 differentiation in multicellular spheroids of human colon carcinoma. *Cancer Res*.  
657 1986;46(10):5320-5329.
- 658 71. Hirschhaeuser F, Menne H, Dittfeld C, West J, Mueller-Klieser W, Kunz-Schughart LA.  
659 Multicellular tumor spheroids: an underestimated tool is catching up again. *J Biotechnol*.  
660 2010;148(1):3-15. doi:10.1016/j.jbiotec.2010.01.012

- 661 72. Cesarz Z, Tamama K. Spheroid Culture of Mesenchymal Stem Cells. Li R-K, ed. *Stem Cells Int.*  
662 2015;2016:9176357. doi:10.1155/2016/9176357
- 663 73. Mueller-Klieser W. Three-dimensional cell cultures: from molecular mechanisms to clinical  
664 applications. *Am J Physiol.* 1997;273(4):C1109-1123. doi:10.1152/ajpcell.1997.273.4.C1109
- 665 74. Foldager CB, Nielsen AB, Munir S, et al. Combined 3D and hypoxic culture improves cartilage-  
666 specific gene expression in human chondrocytes. *Acta Orthop.* 2011;82(2):234-240.  
667 doi:10.3109/17453674.2011.566135
- 668 75. Schrobback K, Malda J, Crawford RW, Upton Z, Leavesley DI, Klein TJ. Effects of oxygen on  
669 zonal marker expression in human articular chondrocytes. *Tissue Eng Part A.* 2012;18(9-  
670 10):920-933. doi:10.1089/ten.TEA.2011.0088
- 671 76. Shi Y, Ma J, Zhang X, Li H, Jiang L, Qin J. Hypoxia combined with spheroid culture improves  
672 cartilage specific function in chondrocytes. *Integr Biol Quant Biosci Nano Macro.*  
673 2015;7(3):289-297. doi:10.1039/c4ib00273c
- 674 77. Greco KV, Iqbal AJ, Rattazzi L, et al. High density micromass cultures of a human chondrocyte  
675 cell line: A reliable assay system to reveal the modulatory functions of pharmacological agents.  
676 *Biochem Pharmacol.* 2011;82(12):1919-1929. doi:10.1016/j.bcp.2011.09.009
- 677 78. Huang AH, Motlekar NA, Stein A, Diamond SL, Shore EM, Mauck RL. High-throughput screening  
678 for modulators of mesenchymal stem cell chondrogenesis. *Ann Biomed Eng.* 2008;36(11):1909-  
679 1921. doi:10.1007/s10439-008-9562-4
- 680 79. Willard VP, Diekman BO, Sanchez-Adams J, Christoforou N, Leong KW, Guilak F. Use of cartilage  
681 derived from murine induced pluripotent stem cells for osteoarthritis drug screening. *Arthritis*  
682 *Rheumatol Hoboken NJ.* 2014;66(11):3062-3072. doi:10.1002/art.38780
- 683 80. Dennis JE, Splawn T, Kean TJ. High-Throughput, Temporal and Dose Dependent, Effect of  
684 Vitamins and Minerals on Chondrogenesis. *Front Cell Dev Biol.* 2020;8.  
685 doi:10.3389/fcell.2020.00092
- 686 81. Mohanraj B, Meloni GR, Mauck RL, Dodge GR. A high-throughput model of post-traumatic  
687 osteoarthritis using engineered cartilage tissue analogs. *Osteoarthritis Cartilage.*  
688 2014;22(9):1282-1290. doi:10.1016/j.joca.2014.06.032
- 689 82. Parreno J, Bianchi VJ, Sermer C, et al. Adherent agarose mold cultures: An in vitro platform for  
690 multi-factorial assessment of passaged chondrocyte redifferentiation. *J Orthop Res Off Publ*  
691 *Orthop Res Soc.* 2018;36(9):2392-2405. doi:10.1002/jor.23896
- 692 83. Ham SL, Atefi E, Fyffe D, Tavana H. Robotic Production of Cancer Cell Spheroids with an  
693 Aqueous Two-phase System for Drug Testing. *J Vis Exp JoVE.* 2015;(98). doi:10.3791/52754
- 694 84. Aijian AP, Garrell RL. Digital microfluidics for automated hanging drop cell spheroid culture. *J*  
695 *Lab Autom.* 2015;20(3):283-295. doi:10.1177/2211068214562002
- 696 85. Friedrich J, Seidel C, Ebner R, Kunz-Schughart LA. Spheroid-based drug screen: considerations  
697 and practical approach. *Nat Protoc.* 2009;4(3):309-324. doi:10.1038/nprot.2008.226

- 698 86. Atefi E, Lemmo S, Fyffe D, Luker GD, Tavana H. High Throughput, Polymeric Aqueous Two-  
699 Phase Printing of Tumor Spheroids. *Adv Funct Mater.* 2014;24(41):6509-6515.  
700 doi:10.1002/adfm.201401302
- 701 87. Beachley VZ, Wolf MT, Sadtler K, et al. Tissue matrix arrays for high-throughput screening and  
702 systems analysis of cell function. *Nat Methods.* 2015;12(12):1197-1204.  
703 doi:10.1038/nmeth.3619
- 704 88. Shahi Thakuri P, Ham SL, Luker GD, Tavana H. Multiparametric Analysis of Oncology Drug  
705 Screening with Aqueous Two-Phase Tumor Spheroids. *Mol Pharm.* 2016;13(11):3724-3735.  
706 doi:10.1021/acs.molpharmaceut.6b00527
- 707 89. Zanoni M, Piccinini F, Arienti C, et al. 3D tumor spheroid models for in vitro therapeutic  
708 screening: a systematic approach to enhance the biological relevance of data obtained. *Sci Rep.*  
709 2016;6(1):19103. doi:10.1038/srep19103
- 710 90. Côrtes I, Matsui RAM, Azevedo MS, et al. A Scaffold- and Serum-Free Method to Mimic Human  
711 Stable Cartilage Validated by Secretome. *Tissue Eng Part A.* Published online May 2, 2019.  
712 doi:10.1089/ten.TEA.2018.0311
- 713 91. Schon BS, Hooper GJ, Woodfield TBF. Modular Tissue Assembly Strategies for Biofabrication of  
714 Engineered Cartilage. *Ann Biomed Eng.* 2017;45(1):100-114. doi:10.1007/s10439-016-1609-3
- 715 92. Mansour, Joseph M. Biomechanics of Cartilage. In: *Kinesiology: The Mechanics and*  
716 *Pathomechanics of Human Movement.* 5th ed. Lippincott Williams and Wilkins; 2004:980.
- 717 93. Mohanraj B, Hou C, Meloni GR, Cosgrove BD, Dodge GR, Mauck RL. A high throughput  
718 mechanical screening device for cartilage tissue engineering. *J Biomech.* 2014;47(9):2130-2136.  
719 doi:10.1016/j.jbiomech.2013.10.043
- 720 94. Ranga A, Gobaa S, Okawa Y, Mosiewicz K, Negro A, Lutolf MP. 3D niche microarrays for  
721 systems-level analyses of cell fate | Nature Communications. *Nat Commun.* 2014;5(1):4324.  
722 doi:10.1038/ncomms5324
- 723 95. Dolatshahi-Pirouz A, Nikkhah M, Gaharwar AK, et al. A combinatorial cell-laden gel microarray  
724 for inducing osteogenic differentiation of human mesenchymal stem cells. *Sci Rep.*  
725 2014;4:3896. doi:10.1038/srep03896
- 726 96. Galuzzi M, Perteghella S, Antonioli B, et al. Human Engineered Cartilage and Decellularized  
727 Matrix as an Alternative to Animal Osteoarthritis Model. *Polymers.* 2018;10(7).  
728 doi:10.3390/polym10070738
- 729 97. Yeung P, Zhang W, Wang XN, Yan CH, Chan BP. A human osteoarthritis osteochondral organ  
730 culture model for cartilage tissue engineering. *Biomaterials.* 2018;162:1-21.  
731 doi:10.1016/j.biomaterials.2018.02.002
- 732 98. Lee J, Jeon O, Kong M, et al. Combinatorial screening of biochemical and physical signals for  
733 phenotypic regulation of stem cell-based cartilage tissue engineering. *Sci Adv.*  
734 2020;6(21):eaaz5913. doi:10.1126/sciadv.aaz5913
- 735 99. Vega SL, Kwon MY, Burdick JA. Recent advances in hydrogels for cartilage tissue engineering.  
736 *Eur Cell Mater.* 2017;33:59-75. doi:10.22203/eCM.v033a05

- 737 100. Vega SL, Kwon MY, Song KH, et al. Combinatorial hydrogels with biochemical gradients for  
738 screening 3D cellular microenvironments. *Nat Commun.* 2018;9(1):614. doi:10.1038/s41467-  
739 018-03021-5
- 740 101. Li Y, Fan Q, Jiang Y, Gong F, Xia H. Effects of insulin-like growth factor 1 and basic fibroblast  
741 growth factor on the morphology and proliferation of chondrocytes embedded in Matrigel in a  
742 microfluidic platform. *Exp Ther Med.* 2017;14(3):2657-2663. doi:10.3892/etm.2017.4808
- 743 102. De Moor L, Fernandez S, Vercruyse C, et al. Hybrid Bioprinting of Chondrogenically Induced  
744 Human Mesenchymal Stem Cell Spheroids. *Front Bioeng Biotechnol.* 2020;8.  
745 doi:10.3389/fbioe.2020.00484
- 746 103. Kolb L, Allazetta S, Karlsson M, Girgin M, Weber W, Lutolf MP. High-throughput stem cell-  
747 based phenotypic screening through microniches. *Biomater Sci.* 2019;7(8):3471-3479.  
748 doi:10.1039/c8bm01180j
- 749 104. Lancaster MA, Huch M. Disease modelling in human organoids. *Dis Model Mech.* 2019;12(7).  
750 doi:10.1242/dmm.039347
- 751 105. Clevers H. Modeling Development and Disease with Organoids. *Cell.* 2016;165(7):1586-1597.  
752 doi:10.1016/j.cell.2016.05.082
- 753 106. Lancaster MA, Renner M, Martin C-A, et al. Cerebral organoids model human brain  
754 development and microcephaly. *Nature.* 2013;501(7467):373-379. doi:10.1038/nature12517
- 755 107. McCracken KW, Catá EM, Crawford CM, et al. Modelling human development and disease in  
756 pluripotent stem-cell-derived gastric organoids. *Nature.* 2014;516(7531):400-404.  
757 doi:10.1038/nature13863
- 758 108. Hu H, Gehart H, Artegiani B, et al. Long-Term Expansion of Functional Mouse and Human  
759 Hepatocytes as 3D Organoids. *Cell.* 2018;175(6):1591-1606.e19. doi:10.1016/j.cell.2018.11.013
- 760 109. O'Connor SK, Katz DB, Oswald SJ, Groneck L, Guilak F. Formation of Osteochondral Organoids  
761 from Murine Induced Pluripotent Stem Cells. *Tissue Eng Part A.* Published online December 22,  
762 2020. doi:10.1089/ten.TEA.2020.0273
- 763 110. Loeser RF, Goldring SR, Scanzello CR, Goldring MB. Osteoarthritis: A Disease of the Joint as an  
764 Organ. *Arthritis Rheum.* 2012;64(6):1697-1707. doi:10.1002/art.34453
- 765 111. Chen D, Shen J, Zhao W, et al. Osteoarthritis: toward a comprehensive understanding of  
766 pathological mechanism. *Bone Res.* 2017;5(1):1-13. doi:10.1038/boneres.2016.44
- 767 112. Rosser J, Bachmann B, Jordan C, et al. Microfluidic nutrient gradient-based three-dimensional  
768 chondrocyte culture-on-a-chip as an in vitro equine arthritis model. *Mater Today Bio.*  
769 2019;4:100023. doi:10.1016/j.mtbio.2019.100023
- 770 113. Occhetta P, Mainardi A, Votta E, et al. Hyperphysiological compression of articular cartilage  
771 induces an osteoarthritic phenotype in a cartilage-on-a-chip model. *Nat Biomed Eng.*  
772 2019;3(7):545-557. doi:10.1038/s41551-019-0406-3
- 773 114. Lin Z, Li Z, Li EN, et al. Osteochondral Tissue Chip Derived From iPSCs: Modeling OA Pathologies  
774 and Testing Drugs. *Front Bioeng Biotechnol.* 2019;7:411. doi:10.3389/fbioe.2019.00411

775 Table 1: 2D screening platforms for cartilage

Authors	Cell type(s)	Model	Chondrogenic medium?	Molecules/ parameters tested	Culture period	Outcomes
Johnson et al. (2012) <sup>29</sup>	Human BMSC	384-well format. Cells seeded in monolayer and molecules added to medium.	No	22,000 structurally diverse, heterocyclic, drug-like molecules (5 $\mu$ M). KGN hit.	4 days	Presence of chondrogenic nodules with rhodamine B staining and light microscopy
Rape et al. (2015) <sup>44</sup>	Human glioblastoma cells and ASC	Combinatorial hydrogels. HA gels with stiffness and fibronectin density gradients cured onto glass slides. Cells seeded on top.	No	Different stiffnesses and fibronectin concentrations	2 days (glioblastoma) and 7 days (hASC)	Cancer model: miR18a expression via fluorescence assay. Adipogenic/osteogenic model: Oil Red O and NBT/BCIP staining.
Floren and Tan (2015) <sup>42</sup>	Rodent BMSC/PASMC	ECM microarray. Electrospun PEGDM and PEO deposited onto glass slides and photopolymerised. Spotted with different ECM proteins. Cells seeded on top	No	Collagen I, collagen III, collagen IV, laminin, fibronectin, elastin	24 hours	Cell adhesion and spreading with DAPI and phalloidin. ICC (PECAM-1 vascular marker). Imaged with automated confocal microscopy
Le et al. (2015) <sup>12</sup>	ATDC5 chondrogenic cell line	96-well format. Cells seeded in monolayer and molecules added to medium.	Yes	LOPAC library of 1280 pharmaceutically active compounds	9 days	Total collagen via fluorescent collagen probe assay.
Choi et al. (2016) <sup>33</sup>	Human ASC	60 mm plates. Cells seeded in monolayer and molecules added to medium.	No	In-house protein kinase inhibitor library of sulphonamides (1 $\mu$ M and 10 $\mu$ M). Compound 6 hit.	11 days	Aggrecan expression via ELISA
Tong et al. (2016) <sup>45</sup>	Human fibroblasts	Combinatorial PEG hydrogels with mechanical and ligand density gradients formed on glass slides and cells seeded on top.	No	Different stiffnesses and RGD binding densities	24 hours	Cell adhesion and morphology, cytoskeleton structure and spreading/elongation all via staining and microscopy

Sharma et al. (2017) <sup>7</sup>	Various, including bovine chondrocytes	PEG hydrogels electrospun onto glass slide and UV cured, then peptide microarray deposited on top via array spotting system. Cells (mono- and co-cultures) seeded on top.	Yes (chondrocytes only)	Multiple peptide motifs and concentrations	24 hours	Cell adhesion and morphology and cytoskeleton structure via staining and confocal microscopy
Ming et al. (2018) <sup>8</sup>	Rodent chondrocytes	Microfluidic device used to create concentration gradient of molecule. 8 concentrations of medium/drug directed to cells cultured in monolayer in 8 downstream chambers.	No	Resveratrol (0-200 $\mu$ M)	3 days	Proliferation via cell counting via light microscopy
Gobaa et al. (2018) <sup>43</sup>	Human BMSC	2016-well format, combinatorial protein array. Proteins deposited onto thin layer of PEG hydrogel via robotic liquid handling system and cells seeded on top.	No	Wnt3a, Wnt5a, DKK1, BMP2, DLL4, Jag, DLK1, NCAM, GDF8, CCL2, laminin Different PEG stiffnesses	11 days	Proliferation with DAPI and phalloidin and adipogenic differentiation with Nile Red staining. Imaged with automated microscopy
Deshmukh et al. (2018) <sup>10</sup>	TCF/LEF reporter cell line and human BMSC	Molecules adhered to multi-well screening plates via robotic liquid handling system and cell seeded on top.	Yes (BMSC only)	Wnt pathway inhibitors: SM04690, FH535, IWR-1, ICG001, iCRT14, KY02111, CX.4945	2 days (TCF/LEF reporters) 5 days (hBMSC)	Luciferase activity (TCF/LEF reporters) Presence of chondrogenic nodules with rhodamine B staining and automated imaging system (hBMSC)
Nogueira-Recalde (2019) <sup>9</sup>	T/C28a2 chondrocyte cell line	384-well format. Cells seeded in monolayer. Aged/senescent model induced with IL-6. Automated cell dispensing and liquid handling.	No	Prestwick chemical library of 1120 approved drugs	Not specified	Senescence-associated- $\beta$ -galactosidase activity via ImaGene Green™ C12FDG lacZ Gene Expression Kit. Autophagy levels via LC3 reporter. Imaged with Operetta® High Content Screening system.
Shi et al. (2019) <sup>11</sup>	Murine chondrogenic cell line	96-well format. Cells seeded in monolayer and molecules added to medium.	No	Library of 2320 natural and synthetic small compounds (10 $\mu$ M). BNTA hit.	5 days	Alcian Blue stain for proteoglycans assessed via light microscopy



776 ASC = adipose-derived stem cell. BMSC = bone marrow stromal cell. ECM = extracellular matrix. ELISA = enzyme-linked immunosorbent assay. HA =

777 hyaluronic acid. ICC = immunocytochemistry. PEG = poly(ethylene glycol). PEO = poly(ethylene oxide). PASMC = pulmonary arterial smooth muscle cells.

778 RGD = Arg-Gly-Asp tri-peptide

779

780 Table 2: 3D screening platforms

Authors	Cell type(s)	Model	Tissue type	Molecules/ parameters tested	Culture period	Outcomes
Huang et al. (2008) <sup>78</sup>	Bovine BMSC	Spheroids. 384-well format via microplate filling system.	Chondrogenic	NINDS library of 1040 compounds	7 days	Automated, in-well DNA and sGAG assays.
Friedrich et al. (2009) <sup>85</sup>	Tumour cell lines	Spheroids. 96-well format via semi-automated multi-channel pipetting system.	Tumour	N/A	7 days	Spheroid growth and integrity via semi-automated microscopy. Proliferation via thymidine incorporation assay.
Willard et al. (2014) <sup>79</sup>	iPSC with <i>COL2A1</i> reporter system	Spheroids. 96-well format.	Chondrogenic	IL-4, TIMP-3, NS-398, SC-514, GM-6001	3 days	Cell number, elastic modulus change, GAG loss, production of MMPs, prostaglandin and NO.
Atefi et al. (2014) <sup>86</sup>	A431.H9 skin cancer cell line	Spheroids. 96-well format via robotic liquid handler and two-phase PEG/dextran system	Tumour	Cisplatin and paclitaxel	7 days	Viability and standard microplate reader-based assays.
Aijan and Garrell (2014) <sup>84</sup>	Murine BMSC, colorectal cancer line, human fibroblasts	Spheroids. Hanging drop culture via digital microfluidics and automated liquid handling system.	Tumour	Insulin and irinotecan (cancer line only)	4 days	Viability and spheroid size via confocal microscopy.
Beachley et al. (2015) <sup>87</sup>	Human cancer cell line	Spheroids. Hanging drop culture.	Tumour	ECM digests from different anatomical locations	11 days	Potential for metabolic assays, single-cell analysis/sorting and gene expression analysis.
Dennis et al. (2020) <sup>80</sup>	ATDC5 chondrogenic cell line	Spheroids. 96-well format.	Chondrogenic	15 vitamins and minerals	21 days	Collagen type II promoter expression via luciferase reporter.
Greco et al. (2011) <sup>77</sup>	C-28/I2 chondrogenic cell line	Micromass. 24-well format.	Chondrogenic	Prednisolone and naproxen	5 days	sGAG assay and gene expression analysis (anabolic/catabolic genes).
Mohanraj et al. (2014) <sup>81</sup>	Bovine chondrocytes	Micromass. 96-well format. Cultured for 14-16 weeks before injurious compression applied. Post-traumatic OA model.	Chondrogenic	NAC, ZVF, Polaxamer 188	5 days	DNA, sGAG and LIVE/DEAD assays. Alcian Blue staining for sGAG.

Parreno et al. (2018) <sup>82</sup>	Bovine chondrocytes (dedifferentiated)	Micromass. 96-well format. Cells seeded onto TCP, confined inside agarose tubes with 3 mm diameter. Combinatorial screen of 3 growth factors.	Chondrogenic	TGFβ-1, FGF2 and FGF18	14 days	Alcian Blue staining for proteoglycan accumulation. Eluted dye quantified via microplate reader.
Ranga et al. (2014) <sup>94</sup>	Murine ESC with OCT4 reporter system	Combinatorial hydrogels. 384-well format. Cells encapsulated in multifactorial PEG-based gels via robotic liquid handling system.	N/A	Mechanical properties, degradability, various proteins and soluble factors	5 days	Colony size, LIVE/DEAD and OCT4 (GFP) expression via automated microscopy. Indentation testing, flow cytometry, PCR.
Dolatshahi-Pirouz et al. (2014) <sup>95</sup>	Human BMSC	Combinatorial hydrogels. Cells encapsulated in GelMA with different combinations of proteins and microgels printed onto glass slides via robotic spotter.	Osteogenic	Fibronectin, laminin, osteocalcin, BMP2 and BMP5	7 or 14 days	Osteogenic model – ALP assay, mechanical testing and mineralisation. OPN expression and Alizarin Red staining via confocal microscopy.
Mohanraj et al. (2014) <sup>93</sup>	Bovine BMSC	Hydrogels. Cell-laden hyaluronic acid set between 2 glass plates and cylindrical constructs punched out.	Chondrogenic	TNF-α	6 days	DNA and sGAG assays. Griess assay for NO production and mechanical testing.
Li et al. (2017) <sup>101</sup>	Rabbit articular chondrocytes	Hydrogels. Cells encapsulated in Matrigel and loaded into perfusion microfluidic device. Combinatorial screen of 2 growth factors.	Chondrogenic	IGF-1 and FGF2	2 weeks	Collagen type II expression via ICF.
Galuzzi et al. (2018) <sup>96</sup>	Human nasal chondrocytes	Multiple: alginate beads, decellularised cartilage, spheroids, silk/alginate microcarriers.	Chondrogenic	IL-1β	15 days	GAG release into medium and metabolic activity.
Yeung et al. (2018) <sup>97</sup>	Human BMSC	Hydrogels. Cells encapsulated in collagen droplets then inserted into human osteochondral grafts.	Chondrogenic	GM6601	4 and 8 weeks	Collagen type II, MMP13 and ADAMTS-5 via ELISA. Histology and IHC.
Vega et al. (2018) <sup>100</sup>	Human BMSC	Combinatorial hydrogels. Cells encapsulated in HA gels with a gradient of tethered peptides.	Chondrogenic	His-Ala-Val motif and RGD	7 days	SOX9 and aggrecan expression via ICF and single cell confocal imaging. Mechanical properties via atomic force microscopy.

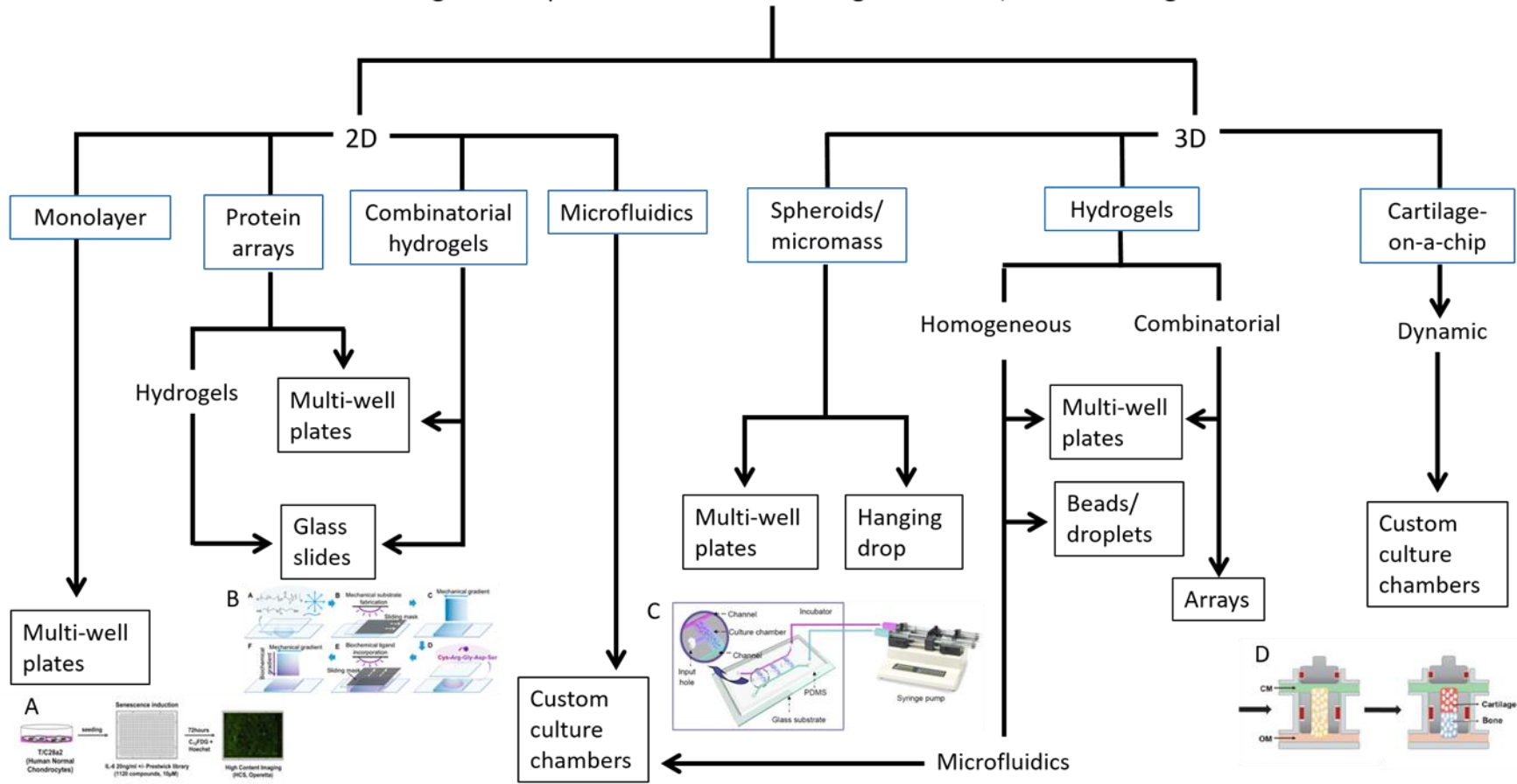
Kolb et al. (2019) <sup>103</sup>	HEK-IL4-YFP reporter cell line	Hydrogels. Combinatorial cell aggregates encapsulated in A) non-degradable PEG followed by B) degradable, protein-functionalised PEG. Microfluidics system.	N/A	IL4, IGF1, BMP2, BMP4, ActA, Wnt3a	8 days	Protein expression via YFP reporter and plate reader. Barcoded RNA sequencing.
Lee et al. (2020) <sup>98</sup>	Human BMSC	Combinatorial hydrogels. Cells encapsulated in PEG/alginate gels of different ratios with and without RGD and/or TGF- $\beta$ 1. 3D printed onto 288 gel array	Chondrogenic	Different compressive strains and TGF- $\beta$ 1 concentrations	7 and 21 days	LIVE/DEAD assay, GAG deposition and degradation. ICF for collagen type II, aggrecan and Runx2 via confocal microscopy. Mechanical testing.
Occhetta et al. (2019) <sup>113</sup>	Human articular chondrocytes	Cartilage-on-a-chip. Cell-laden PEG hydrogels cast into PDMS microchambers at branched ends of moulds with central channel for medium exchange. Compression applied to create OA model.	Chondrogenic	Dexamethasone, IL-1Ra, rapamycin, celecoxib, HYADD 4 and HA	24 days	DNA and sGAG assay. Gene expression (panel of genes). ICF for aggrecan, collagen types I and II, MMP-13 and DIPEN. MMP-13 release via assay kit.
Rosser et al. (2019) <sup>112</sup>	Equine chondrocytes	Cartilage-on-a-chip, microfluidic device. Fibrin-encapsulated cells pipetted into semi-circular chambers. Medium forced past flat part of semicircle only, to generate joint-mimicking cyclic shear stress and concentration gradients.	Chondrogenic	TNF- $\alpha$ and IL-1 $\beta$	7 and 21 days	LIVE/DEAD and metabolic activity assays. Gene expression analysis for <i>COL2A1</i> , <i>ACAN</i> , <i>SOX9</i> . Histology and IHC.
Lin et al. (2019) <sup>114</sup>	iPSC	Osteochondral tissue chip. Gelatin-encapsulated in gelatin pipetted into custom inserts. Dual flow bioreactor delivers two types of media (top and bottom).	Chondrogenic and osteogenic	Celecoxib	35 days	Gene expression analysis (anabolic/chondrogenic, catabolic and inflammatory markers).
Peck et al. (2017) <sup>115</sup>	Porcine chondrocytes, synovial cell line and macrophages (activated THP-1 cells)	Scaffold free. 24-well plate format. Chondrocyte-laden gelatin microspheres encapsulated in alginate. Gelatin dissolved to leave cells in cavities. After 35 days alginate removed and synovial cells added to remaining tissue nodules. Macrophages added the following day.	Chondrogenic	Celecoxib	7 days (tri-culture)	Gene expression analysis (apoptotic, anabolic, inflammatory, chondrogenic). Histology for GAGs. Proliferation.

781 ALP = alkaline phosphatase. BMSC = bone marrow stromal cells. ECM = extracellular matrix. ELISA = enzyme-linked immunosorbent assay. ESC = embryonic

782 stem cell. GAG = glycosaminoglycan. GelMA = gelatin methacrylate. GFP = green fluorescent protein. HA = hyaluronic acid. HEK = human embryonic kidney.

783 ICF = immunocytofluorescence. ICH = immunohistochemistry. IL4 = interleukin 4. iPSC = induced pluripotent stem cell. MMP = matrix metalloproteinase.  
784 NINDS = National Institute of Neurological Disorders and Stroke. NO = nitrous oxide. OA = osteoarthritis. PDMS = polydimethylsiloxane. PEG = poly(ethylene  
785 glycol). PCR = polymerase chain reaction. RGD = Arg-Gly-Asp tri-peptide. sGAG = sulphated glycosaminoglycan. YFP = yellow fluorescent protein.

### Cartilage model platforms for the screening of anabolic/catabolic drugs



786

787 Figure 1. Schematic of existing 2D and 3D drug screening platforms for cartilage and tissues of a similar lineage. 335x183mm (150 x 150 DPI)